

**Direct measurement
of ozone production
rates in Houston**

M. Cazorla et al.

**Direct measurement of ozone production
rates in Houston in 2009 and comparison
with two estimation methods**

M. Cazorla^{1,*}, W. H. Brune¹, X. Ren^{2,}, and B. Lefer³**

¹Department of Meteorology, Pennsylvania State University, University Park, PA, USA

²Rosentiel School of Marine and Atmospheric Science, University of Miami, FL, USA

³Department of Earth and Atmospheric Sciences, University of Houston, Houston, TX, USA

* now at: Atmospheric Chemistry and Dynamics Branch, NASA Goddard Space Flight Center, Greenbelt, MD, USA

** now at: Air Resources Laboratory, National Oceanic and Atmospheric Administration, Silver Spring, MD, USA

Received: 22 September 2011 – Accepted: 23 September 2011 – Published: 10 October 2011

Correspondence to: M. Cazorla (cazorla.chem@gmail.com)

Published by Copernicus Publications on behalf of the European Geosciences Union.

[Title Page](#)

[Abstract](#) [Introduction](#)

[Conclusions](#) [References](#)

[Tables](#) [Figures](#)

[⏪](#) [⏩](#)

[◀](#) [▶](#)

[Back](#) [Close](#)

[Full Screen / Esc](#)

[Printer-friendly Version](#)

[Interactive Discussion](#)



Abstract

Ozone production rates, $P(O_3)$, were measured directly using the Penn State Measurement of Ozone Production Sensor (MOPS) during the Study of Houston Atmospheric Radical Precursors (SHARP 2009). Measured $P(O_3)$ peaked in the late morning, with values between 15 ppbv h^{-1} and 100 ppbv h^{-1} , although values of $40\text{--}80 \text{ ppbv h}^{-1}$ were typical for higher ozone days. These measurements were compared against ozone production rates calculated using measurements of hydroperoxyl (HO_2), hydroxyl (OH), and nitric oxide (NO) radicals, called “calculated $P(O_3)$ ”. The same comparison was done using modeled radicals obtained from a box model with the RACM2 mechanism, called “modeled $P(O_3)$ ”. Measured and calculated $P(O_3)$ had similar peak values but the calculated $P(O_3)$ tended to peak earlier in the morning when NO values were higher. Measured and modeled $P(O_3)$ had a similar dependence on NO, but the modeled $P(O_3)$ was only half the measured $P(O_3)$. This difference indicates possible missing radical sources in the box model with the RACM2 mechanism and thus has implications for the ability of air quality models to accurately predict ozone production rates.

1 Introduction

The environmental community has been holding a debate with regard to lowering the Ambient Air Quality Standards for ozone (O_3) from 75 ppbv to a new level between $60\text{--}70 \text{ ppbv}$ (EPA, 2010). The new ozone standard will be reconsidered in 2013. At present, if the standard were set to 70 ppbv , the increment in the number of counties nationwide in non-attainment would be 50 % with respect to the current number (342). If the standard were set to 60 ppbv , the increment would be 90 % (McCarthy, 2010).

Areas already designed as being in non-attainment with the current ozone standard such as Houston-Galveston-Brazoria, would face a more difficult challenge under new rules. As an example, during the month of May 2009, the Texas Commission

Direct measurement of ozone production rates in Houston

M. Cazorla et al.

Title Page

Abstract

Introduction

Conclusions

References

Tables

Figures

⏪

⏩

◀

▶

Back

Close

Full Screen / Esc

Printer-friendly Version

Interactive Discussion



on Environmental Quality (2011) reported four cases of exceedances of the current primary ozone standard in Houston.

Future controls in ozone precursors, namely NO_x and VOCs, from mobile and point sources will be more exigent with stricter standards. As a result, the need to monitor locally not only ambient ozone but the actual ozone production rate is becoming increasingly important.

Ambient ozone is the result of local photochemical production, surface deposition, and transport processes. The amount of ground-level ozone can be easily obtained from a direct measurement using a commercial ozone analyzer. These ambient ozone measurements, however, do not indicate whether ozone is locally produced or imported from other areas. Thus the relationship between ozone and its precursors cannot be obtained from simple ambient ozone measurements alone. Typically, an air quality model that includes emissions, transport, and chemistry is used to link ozone to its precursors, but emissions inventories and transport are both uncertain (Fox, 1984; NRC, 1991; Gilliland et al., 2008).

The Measurement of Ozone Production Sensor, MOPS, whose functioning and operation is detailed in Cazorla and Brune (2010), monitors in real time the rate of photochemical production of ozone, $P(\text{O}_3)$, in the ambient air. In addition, sensitivity of $P(\text{O}_3)$ to precursors can be investigated under real conditions with this instrument. The data retrieved from the MOPS will contribute to a solid scientific basis for designing air quality regulations and emission controls. Another important benefit of using this new monitor is the ability to quantify local production versus transport of ozone, in particular if a network of these instruments is located along the path of meteorological features that are associated with ozone advection.

The chemistry of ozone production has been presented in a thorough manner by several authors (Haagen-Smit et al., 1953; Finlayson-Pitts and Pitts, 1977; Logan et al., 1981; Gery et al., 1989; Kleinman, 2005; Seinfeld and Pandis, 2006). The current understanding of the ozone-forming chemistry indicates that the photolysis of nitrogen dioxide (NO_2) is the only known source of ozone in the daytime. In the absence of

Direct measurement of ozone production rates in Houston

M. Cazorla et al.

Title Page

Abstract

Introduction

Conclusions

References

Tables

Figures

◀

▶

◀

▶

Back

Close

Full Screen / Esc

Printer-friendly Version

Interactive Discussion



Direct measurement of ozone production rates in Houston

M. Cazorla et al.

Title Page

Abstract

Introduction

Conclusions

References

Tables

Figures

◀

▶

◀

▶

Back

Close

Full Screen / Esc

Printer-friendly Version

Interactive Discussion



peroxy radicals (HO_2 and RO_2), nitric oxide (NO), nitrogen dioxide (NO_2) and ozone (O_3) achieve photosteady state (PSS) and no new ozone is formed. New ozone is formed by NO_2 formation via reactions of peroxy radicals and NO. Peroxy radicals come from reaction sequences that continuously cycle OH, RO_2 , and HO_2 radicals; these sequences are fast enough that the steady state of the HO_x species can be assumed. The estimation of the rate of ozone production, $P(\text{O}_3)$, from measurements requires the knowledge of the abundance of peroxy radicals and NO present in the ambient air.

The chemical production and loss of ozone as a function of NO_x and VOCs can be represented by the kinetic rate equations. Equation (1) summarizes the production of NO_2 . The k terms are the reaction rate coefficients and the terms in brackets are the concentration of chemical species. The two terms on the right-hand side of Eq. (1) indicate production of NO_2 , and therefore of ozone, from peroxy radicals reacting with NO. Equation (2) represents the paths for ozone loss. The first term on the right-hand side corresponds to ozone loss due to the formation of nitric acid, the second term is the loss due to ozone reacting with HO_2 , and the last term corresponds to organic nitrate production. The net production of ozone results from the difference between chemical production and chemical loss, as shown by Eq. (3).

$$P(\text{O}_3) = k_{\text{HO}_2 + \text{NO}}[\text{HO}_2][\text{NO}] + \sum k_{\text{RO}_2i + \text{NO}}[\text{RO}_2i][\text{NO}] \quad (1)$$

$$I(\text{O}_3) = k_{\text{OH} + \text{NO}_2 + \text{M}}[\text{OH}][\text{NO}_2][\text{M}] + k_{\text{HO}_2 + \text{O}_3}[\text{HO}_2][\text{O}_3] + P(\text{RONO}_2) \quad (2)$$

$$P(\text{O}_3) = p(\text{O}_3) - I(\text{O}_3) \quad (3)$$

In addition to calculations using ancillary measurements, the estimation of the rate of ozone production has been traditionally done by chemical modeling. In this study, we use the Regional Atmospheric Chemistry Mechanism Version 2, RACM2, (Goliff and Stockwell, 2008; Goliff and Stockwell, 2010). Past studies have found discrepancies between model results and calculated ozone production rates (Martinez et al., 2003; Ren et al., 2003, 2004; Shirley et al., 2006; Kanaya et al., 2007). These differences

Direct measurement of ozone production rates in Houston

M. Cazorla et al.

Title Page

Abstract

Introduction

Conclusions

References

Tables

Figures

◀

▶

◀

▶

Back

Close

Full Screen / Esc

Printer-friendly Version

Interactive Discussion



have been attributed to the underprediction of HO₂ by the models. Recent studies by Hofzumahaus et al. (2009) suggest a mechanism for the production of OH that maintains the ratio HO₂/OH and does not involve the reaction of HO₂ with NO and, therefore, does not result in the production of ozone at low NO levels. This mechanism is not included in the traditional models and calculations but can be investigated by monitoring in real time the rate of ozone production.

In this study we use direct measurements of ozone production rates observed in Houston in 2009 to compare against ozone production rates calculated from measured HO₂, OH, and NO radicals and from modeled radicals. The three different methods for obtaining the ozone production rate are compared as a function of time of day as well as a function of NO.

2 Experimental and methods

2.1 Measured $P(O_3)$ and description of the SHARP campaign

The sampling site for the Study of Houston Atmospheric Radical Precursors, SHARP 2009, was the roof of Moody Tower South located at University of Houston. It is 70 m above the ground level and 5 km away from downtown Houston. A fairly complete suite of atmospheric chemical species and meteorological parameters were measured. The measurements used for this study are described below.

The Penn State MOPS (Cazorla and Brune, 2010), was deployed during the SHARP campaign between 15 April and 31 May 2009. The MOPS measures $P(O_3)$ by finding the differential ozone between a transparent chamber and a chamber covered with a UV-blocking film that continuously sample ambient air and are exposed to the sun. An NO₂-to-O₃ converter between the chambers and the ozone monitor accounts for the differences in PSS between the sample and reference chambers by converting NO₂ to O₃ so that the sum of NO₂ and O₃ is measured as O₃. The uncertainty of the MOPS is 30 % at the 2 σ confidence level and 10-min integration time. A complete description of the instrument can be found in Cazorla and Brune (2010). MOPS data is available for 20 days out of the 42-day intensive SHARP study.

**Direct measurement
of ozone production
rates in Houston**

M. Cazorla et al.

Title Page

Abstract

Introduction

Conclusions

References

Tables

Figures

◀

▶

◀

▶

Back

Close

Full Screen / Esc

Printer-friendly Version

Interactive Discussion



OH and HO₂ radicals were measured by the Ground-based Tropospheric Hydrogen Oxides Sensor, GTHOS. The instrument and its calibration have been described in detail in Faloon et al. (2004); an abbreviated description is given here. The detection technique uses laser-induced fluorescence (LIF) at low pressure, often called FAGE (Hard et al., 1984). Ambient air is pulled into a low-pressure chamber with a vacuum pump. As the air flows through the detection chamber, OH radicals are excited by the laser and their resultant fluorescence is detected at a wavelength near 308 nm. HO₂ is chemically converted to OH by the reaction with reagent NO followed by LIF detection of OH in a second detection axis. The detection limits are about 0.02 parts per trillion volume (pptv) for OH for a 20-min integration time and 0.1 pptv for HO₂ with a 2σ confidence level and 1-min integration time. Estimated absolute uncertainty at the 2σ confidence level is ±32 % for both OH and HO₂ (Faloon et al., 2004).

Ambient ozone (2.2 % uncertainty), NO and NO₂ (5.7 % uncertainty), SO₂ and CO (5.5 % uncertainty), meteorological data and photolysis rate coefficients (less than 12 % uncertainty) were monitored by the University of Houston (Lefer et al., 2010) on a tower about six meters away from the MOPS. NO and NO₂ were also measured by NOAA instruments that were co-located with the University of Houston instruments (Luke et al., 2010). In addition, NO was measured with a Penn State Thermo 42C NOx monitor (6 % uncertainty) connected to the MOPS data acquisition. The comparison of the MOPS NO measurements with those from NOAA showed good agreement, with a slope of 0.98 and an intercept of 0.15 ppbv. This agreement indicates that all the instruments were sampling basically the same air masses despite the slight separation in the measurement inlets for the different species.

Volatile organic compounds (C₂–C₁₀) were measured by University of Houston (5.4 % and 10.2 % uncertainty for alkanes and alkenes, respectively) with a gas chromatographic system coupled to a flame ionization detector (GC-FID) (Leuchner and Rappenglück, 2010). Other organic compounds were measured by Washington State University with a PTR-MS (20 % uncertainty) (Jobson et al., 2005).

Uncertainties in the measurements are listed also in Chen et al. (2010).

Thus, all of the chemical species needed to model and calculate $P(O_3)$ were measured during SHARP. The specific computations for each case are explained in the following sections.

2.2 $P(O_3)$ obtained from modeled radicals (called modeled $P(O_3)$)

The modeled concentrations of the radicals HO_2 , RO_2 , and OH were used in Eqs. (1)–(3) to compute $P(O_3)$. Modeled radicals came from runs of a box model using RACM2 which is an updated version of RACM (Stockwell et al., 1997). The main updates include new oxidation schemes for isoprene and aromatics (benzene, toluene and xylenes). Some organic species such as acetone, acetaldehyde, and methyl vinyl ketone are treated explicitly. A few new reactions such as the photolysis of benzaldehyde and glyoxal and organic acids + OH were added. The RACM2 mechanism includes 356 reactions and 117 total species, including 17 stable inorganic species, 4 inorganic intermediates, 54 stable organic species (4 of these are primarily of biogenic origin) and 42 organic intermediates (Goliff and Stockwell, 2008; Goliff and Stockwell, 2010).

In the present study, atmospheric constituents and environmental parameters were used to constrain the model. The contribution of RO_2 radicals to ozone production was computed from individual peroxy radicals calculated in the RACM2 mechanism, i.e. $P(O_3)_{RO_2} = \sum k_{RO_2j+NO} \cdot [RO_{2j}] \cdot [NO]$. The RO_2 species included in the sum were from oxidation of alkanes, alkenes, benzene, toluene and less reactive aromatics, m,p-xylene, o-xylene, biogenic alkenes, acetone, methyl ethyl ketone, other ketones, methacrolein, methyl vinyl ketone, unsaturated aldehydes, benzaldehydes, adducts from cresol, methyl catechol, formic acid, and NO_3 -alkene adducts. The contribution to $P(O_3)$ from these RO_2 radicals is typically 1 to 8 ppbv h^{-1} , peaking at noon and is about half of the total modeled $P(O_3)$.

Chemical losses due to the production of nitric acid (first term on the right-hand side of Eq. 2) via reaction of OH and NO_2 are typically 10% of the chemical ozone production. The reaction of HO_2 with O_3 (second term of Eq. 2) has a smaller impact, less than 1% of the total chemical production. The modeled $P(O_3)$ reported here

27527

Direct measurement of ozone production rates in Houston

M. Cazorla et al.

Title Page

Abstract

Introduction

Conclusions

References

Tables

Figures

◀

▶

◀

▶

Back

Close

Full Screen / Esc

Printer-friendly Version

Interactive Discussion



comes from the net balance between the total chemical production minus chemical loss as in Eq. (3).

Chen et al. (2010) determined the uncertainty for modeled $P(\text{O}_3)$ at the 1σ confidence level with 2006 data in Houston. These uncertainties were calculated for different hours of the day and for different pollution scenarios, following the Monte Carlo method (Carslaw et al., 1999) and include uncertainties in rate coefficients, product yields, and measurements. In this study we use the model uncertainties determined by Chen et al. (2010) which correspond to 58 % at 08:00 CST, 24 % at 12:00, 22 % at 14:00 and 81 % at 23:00.

2.3 $P(\text{O}_3)$ calculated from measured radicals (called calculated $P(\text{O}_3)$)

The instantaneous ozone production was also calculated from the measured radicals HO_2 , OH , NO , and NO_2 using Eqs. (1)–(3). RO_2 was not measured, so RO_2 from the RACM2 model run was used.

A recent laboratory study suggests that the HO_2 measurements in some FAGE-type instruments are susceptible to an interference from RO_2 species that come from alkenes (Fuchs et al., 2011). A laboratory study of GTHOS showed that it too had this interference. Compared to HO_2 , the yields for RO_2 are 0.68 for isoprene, 0.66 for ethene, 0.40 for cyclohexane, and 0.54 for α -pinene. The yields from more alkenes and aromatics are still needed, but a yield of 0.60 ± 0.15 is consistent with all species that have been measured so far. Measured HO_2 was thus corrected by $0.6 \cdot \text{RO}_2$ from alkenes + aromatics and then $P(\text{O}_3)$ was calculated in the same way as for the modeled radicals, replacing the modeled HO_2 and OH with measured HO_2 and OH .

The absolute uncertainty of the GTHOS measurement of HO_2 was determined to be $\pm 32\%$ at the 2σ confidence limit (Faloona et al., 2004). However, this new revelation about the alkene-based RO_2 interference increases that uncertainty. Typical midday radical mixing ratios are 18 pptv for measured HO_2 and 4 pptv for modeled alkene-based RO_2 . Using propagation of error, the overall 2σ uncertainty of real HO_2 is $\pm 35\%$

Direct measurement of ozone production rates in Houston

M. Cazorla et al.

Title Page

Abstract

Introduction

Conclusions

References

Tables

Figures

◀

▶

◀

▶

Back

Close

Full Screen / Esc

Printer-friendly Version

Interactive Discussion



for midday conditions. The 2σ uncertainty for $P(\text{O}_3)$ calculated from measured HO_2 and OH is slightly higher at an estimate of $\pm 40\%$, or $\pm 20\%$ at 1σ uncertainty.

3 Results

3.1 Time series of $P(\text{O}_3)$ measurements and calculations

A time series shows the general behavior of the 10-min calculated, measured and modeled $P(\text{O}_3)$ and ambient ozone levels during SHARP (Fig. 1). The measured $P(\text{O}_3)$ obtained using the MOPS shows the expected diurnal variations for $P(\text{O}_3)$, although the peak values vary day to day. The MOPS started measuring on 29 April 2009 and measured $P(\text{O}_3)$ on 20 days. Much of the MOPS data loss was due to cloudiness and rain showers, especially in the first half of May. Data gaps in the GTHOS measurements and in the observations needed for the model reduced the total number of days with overlap of $P(\text{O}_3)$ from measurements and calculations (using radicals and model) to 12. The pollution conditions on these 12 days varied enough that statistical analyses can be applied to the comparison of the different methods.

In early May, high northward winds, considerably cloudiness, and morning or afternoon showers suppressed ozone production as well as ozone. With the exception of 4 May, $P(\text{O}_3)$ did not exceed 25 ppbv h^{-1} and ozone did not exceed 50 ppbv.

More polluted conditions occurred later in the study. The meteorological conditions on 4, 19, 20 and 21 May were such that high data quality was obtained with the MOPS. The afternoon temperatures peaked at near 30°C and the sky was clear. The wind speed was low in the morning, between 1 m s^{-1} and 4 m s^{-1} blowing from the N, NE directions, and the relative humidity ranged between 30–50 % at noon. These conditions were optimal for ozone formation and accumulation in the air. Additionally, there was low relative humidity during the early mornings and nights. Low humidity minimizes the artifact that affects the MOPS (Cazorla and Brune, 2010) and thus the effects of the known interference due to NO_2 loss were negligible. The Texas Commission on

Direct measurement of ozone production rates in Houston

M. Cazorla et al.

Title Page

Abstract

Introduction

Conclusions

References

Tables

Figures



Back

Close

Full Screen / Esc

Printer-friendly Version

Interactive Discussion



Environmental Quality (2011) reported officially that 4, 20 and 29 May were pollution events. Ambient ozone on these days surpassed 80 ppbv and the peak $P(O_3)$ measured with the MOPS was higher than 40 ppbv h^{-1} .

There are three anomalies to note in the data set. First on 29 May, the MOPS registered a spike of 110 ppbv h^{-1} for about an hour at 11:00 that came down below 60 ppbv h^{-1} in the afternoon. This spike was unique in the MOPS data, for which typical peak $P(O_3)$ values were in the 40–80 ppbv h^{-1} range when ozone was high. This spike cannot be explained by any of the other measurements.

Second, on 30 May, both the measured and calculated $P(O_3)$ register a spike of ozone production at 07:00. The MOPS measured 45 ppbv h^{-1} while the calculation yields about 80 ppbv h^{-1} . This spike is not apparent in the modeled results. On this day, the campaign of measurements for the MOPS ended and afternoon data are not available.

Third, the MOPS measured negative rates of ozone production between 0 and 10 ppbv h^{-1} in some early mornings and some evenings. Two explanations come to mind. First, net $P(O_3)$ can be negative if the loss terms in Eq. (2) are larger than the production terms in Eq. (1). The sample chamber has the radical chemistry to produce nitric acid from $OH + NO_2$ while the reference chamber does not. The model, however, never shows net $P(O_3)$ to be negative because if there is sufficient photolysis to produce OH , then there is also sufficient photolysis to produce NO from NO_2 , thus keeping net $P(O_3)$ positive.

It is more likely that NO_2 is preferentially lost in the sample chamber by wall reactions that speed up at higher relative humidities (Wainman et al., 2001). The temperature in the sample chamber was generally found to be less than the temperature in the reference chamber, so that the relative humidity would have been greater in the sample chamber than the reference chamber since both had the same absolute water vapor. Experimental evidence was found for these losses and is explained in Cazorla and Brune (2010).

Direct measurement of ozone production rates in Houston

M. Cazorla et al.

Title Page

Abstract

Introduction

Conclusions

References

Tables

Figures

⏪

⏩

◀

▶

Back

Close

Full Screen / Esc

Printer-friendly Version

Interactive Discussion



**Direct measurement
of ozone production
rates in Houston**

M. Cazorla et al.

Title Page

Abstract

Introduction

Conclusions

References

Tables

Figures

◀

▶

◀

▶

Back

Close

Full Screen / Esc

Printer-friendly Version

Interactive Discussion



Despite these few anomalies, the variation in the $P(\text{O}_3)$ measured by the MOPS is qualitatively consistent with the variation in daily peak ozone and with the $P(\text{O}_3)$ calculated with the modeled radicals and the measured radicals. On days when the peak measured $P(\text{O}_3)$ is high, the O_3 peak is high later in the day. When the peak measured $P(\text{O}_3)$ is low, the O_3 peak is also low. This rough consistency suggests that chemical production of O_3 dominates over transport of O_3 for this Moody Tower site.

3.2 Comparison between measured, calculated and modeled $P(\text{O}_3)$

Measured, calculated and modeled $P(\text{O}_3)$ were compared for overlapping points and only during daylight hours from 05:00 to 20:00 (Fig. 2). Day-to-day variations as well as instrument precision contribute to the scatter in the individual 10-min data points. The median diurnal variation lines (mdv) with 1σ error bars, based on measurement uncertainties for the MOPS and GTHOS instruments as well as model uncertainties, provides visual clues for the similarities and differences among the three methods for obtaining $P(\text{O}_3)$.

Between 12:00 and 20:00 the mdv curves for the three sets of data generally have overlapping error bars, indicating that the three methods agree on $P(\text{O}_3)$. From the mdv curves, the modeled $P(\text{O}_3)$ is both lower and greater than measured $P(\text{O}_3)$ whereas the calculated $P(\text{O}_3)$ is always greater than the modeled $P(\text{O}_3)$. In this time period, however, the differences are not statistically significant.

The main differences among the three methods occur in the morning between 5:00 and noon. At 06:30 the calculated $P(\text{O}_3)$ shows a peak of ozone production of 16 ppbv h^{-1} while the levels of measured and modeled $P(\text{O}_3)$ remain below 3 ppbv h^{-1} . This difference comes from the high morning points for calculated $P(\text{O}_3)$ that occurred mainly on 20, 21 and 30 May.

Between 07:00 and noon, the measured and calculated $P(\text{O}_3)$ are generally in agreement and both are about a factor of two greater than the modeled $P(\text{O}_3)$. These differences are marginally statistically significant. In addition, the calculated $P(\text{O}_3)$ tends to be the largest of the three in the early morning between 05:00 and 09:00,

while the measured $P(O_3)$ tends to be largest from 09:00 to 12:00. Thus, the calculated $P(O_3)$ peaks earliest at 08:00 to 09:00, the measured $P(O_3)$ peaks next at 10:00 to 11:00, and the modeled $P(O_3)$ peaks last at 12:00. These differences in the peak $P(O_3)$ will be discussed in more detail below in the section on the NO-dependence of $P(O_3)$.

3.3 Bias and errors

The ozone production rates can be subjected to the same kinds of statistical analyses that are used to discuss the performance of air quality models. The linear regressions between modeled and calculated $P(O_3)$ versus MOPS measurements are shown in Fig. 3a and b, respectively.

The root mean square error (RMSE), mean bias error (MBE) and the index of agreement (IA) (Willmott, 1981; Appel et al., 2007) have been determined in order to compare each pair of data sets. The RMSE is the average error between model estimations and observations. The MBE contains only the difference between the mean of the model estimations and the mean of the observations. Both RMSE and MBE have the units of the observed or estimated variables. In contrast, the index of agreement is a measurement of the degree of error in model estimations and its values range between 0 and 1, with 1 corresponding to a perfect match.

Equations (4) to (6) contain the expressions used to compute these statistical indices.

$$\text{RMSE} = \sqrt{\frac{\sum_i^N (e_i - o_i)^2}{N}} \quad (4)$$

$$\text{MBE} = \frac{\sum_i^N (e_i - o_i)}{N} \quad (5)$$

Direct measurement of ozone production rates in Houston

M. Cazorla et al.

Title Page

Abstract

Introduction

Conclusions

References

Tables

Figures

◀

▶

◀

▶

Back

Close

Full Screen / Esc

Printer-friendly Version

Interactive Discussion



$$IA = 1 - \frac{\sum_i^N (e_i - o_i)^2}{\sum_i^N (|e_i - \bar{o}_i| + |o_i - \bar{o}|)^2} \quad (6)$$

In these equations the e term stands for “estimation”, which corresponds either to the modeled or the calculated $P(O_3)$; the o term represents “observation”, which corresponds to the MOPS measurements; and finally, N is the number of data pairs compared. In the present case N is 4230, for overlapping points among the three sets of data and for daylight hours only between 05:00 and 20:00.

The correlation coefficients R^2 for the linear regression shown in Fig. 3a and b, are 0.4 for the modeled versus measured $P(O_3)$ and 0.34 for the calculated versus measured $P(O_3)$. The slope of the regression, however, is better for the calculated versus measured $P(O_3)$ with a value of 0.56 as opposed to the modeled versus measured $P(O_3)$ whose slope is only 0.29 indicating underestimated modeled results. The error in the slope and intercept in the linear fits are 1.38 % and 32.5 % for Fig. 3a, and 3.05 % and 71.6 % for Fig. 3b. The index of agreement is slightly better for the calculated versus measured $P(O_3)$ at 0.75 than for the modeled versus measured $P(O_3)$ at 0.65.

The RMSE was calculated using directly the 10-min $P(O_3)$ from measurements and from calculations using measured or modeled radical values. This calculation was done in this way with the purpose of determining the average error of the two estimated $P(O_3)$ data sets with respect to the measurements. In both cases the RMSE is comparable, 14.1 ppbv h⁻¹ for the model and 14.5 ppbv h⁻¹ for the calculation of $P(O_3)$. This similarity between the RMSE for the calculated and modeled $P(O_3)$ is misleading because the peak modeled $P(O_3)$ did not surpass 35 ppbv h⁻¹ during high ozone production episodes, while the calculated and measured $P(O_3)$ show values above 80 ppbv h⁻¹ for the same time period (Fig. 1).

Direct measurement of ozone production rates in Houston

M. Cazorla et al.

Title Page

Abstract

Introduction

Conclusions

References

Tables

Figures

◀

▶

◀

▶

Back

Close

Full Screen / Esc

Printer-friendly Version

Interactive Discussion



In terms of mean bias error the modeled $P(O_3)$ has a negative overall bias of -6 ppbv h^{-1} with respect to the MOPS measurements. This result confirms strong underestimation of the predicted modeled values for the majority of the data with respect to the actual measurements. In contrast, the calculated $P(O_3)$ has a much lower bias of 0.42 ppbv h^{-1} with respect to the measurements. This low MBE comes from the closeness in the calculated $P(O_3)$ to the measured $P(O_3)$ in particular when the ozone production was high. For such cases, the model had considerably lower values of $P(O_3)$ with peak values consistently shifted to later in the day.

The MBE and RMSE of the calculated and modeled $P(O_3)$ versus the measured $P(O_3)$ vary during the day (Fig. 4a and b). The number of binned pairs of data is indicated on top of the x-axis. For the modeled values, the mean bias is negative for the entire set of data. The largest difference for the modeled $P(O_3)$ versus measured $P(O_3)$ occurs between 08:00 and 12:00 when the production of ozone according with MOPS measurements is the largest. The calculated $P(O_3)$, conversely, is large compared to the measured $P(O_3)$ in the early morning before 09:00, whereas between 10:00 and 16:00, when the data are more abundant, the mean bias fluctuates around 0.

In similar manner, the RMSE is strongly different between the two methods in the morning until noon. For the modeled values, the RMSE starts low (7 ppbv h^{-1}) at 06:00 and then increases. For the calculated versus measured $P(O_3)$, the RMSE starts with values higher than 18 ppbv h^{-1} , then the RMSE for the calculated versus measured $P(O_3)$ generally remains between 10 ppbv h^{-1} and 14 ppbv h^{-1} .

These MBE's and RMSE's are driven in part by the precision of the measurements as well as by true differences in the methods for determining $P(O_3)$. Large variations in measured, calculated, and modeled $P(O_3)$ are clear in Figs. 1 and 2. Thus, part of the MBE and RMSE can be attributed to as-yet-unknown factors that could be affecting the MOPS measurements. The biases of the calculated and modeled $P(O_3)$ relative to the measured $P(O_3)$ are, however, clearly different and reflect differences between these two estimation methods.

**Direct measurement
of ozone production
rates in Houston**

M. Cazorla et al.

Title Page

Abstract

Introduction

Conclusions

References

Tables

Figures

◀

▶

◀

▶

Back

Close

Full Screen / Esc

Printer-friendly Version

Interactive Discussion



3.4 Real-time $P(O_3)$ in NO space

The dependence of measured $P(O_3)$ on measured NO evolves over the period from 19 May to 21 May, a period of high pollution (Fig. 5). Peak $P(O_3)$ measured with the MOPS reached 60 ppbv h^{-1} on 19 May, a higher value of 75 ppbv h^{-1} on 20 May, and then peaked at a lower value of 40 ppbv h^{-1} on 21 May. These relative $P(O_3)$ values are consistent with the relative O_3 values for the same days (Fig. 1).

The plotted data in Fig. 5 are the 10-min MOPS data without any smoothing or correction. Reading the plots from right to left, using the hour of the day given by the color scale, it is clear that the curves start with high NO and low $P(O_3)$ before 08:00, grow rapidly as NO falls past the rush hour, reach broad peaks at around 10:00 when NO ranges between 2–10 ppbv, and finally decrease in the afternoon and evening as NO and other radicals decrease. Note particularly that the peak ozone production occurs at mid to high levels of NO, about 10:00, and that the higher the daily peak $P(O_3)$ was, the higher NO for the peak $P(O_3)$.

A comparison for the entire data sets for the measured, calculated, and modeled $P(O_3)$ as a function of NO are shown in Fig. 6, but only for times when all three methods are available and only for times between 05:00 and 20:00. Not all measured $P(O_3)$ shown in Fig. 5 appear in Fig. 6 because there were no calculated or modeled $P(O_3)$ points for some of the measured $P(O_3)$ points in Fig. 5 and only overlapping points for all three methods are shown in Fig. 6.

A first observation from Fig. 6 is that modeled $P(O_3)$ values are low compared to the measurements and the calculations. For the same hour of the day and the same NO levels, the modeled $P(O_3)$ is substantially lower than the measured and calculated $P(O_3)$ suggesting a potential lack of a source of radicals in the model. Moreover, there is rough agreement between the measured and calculated $P(O_3)$ for the magnitude of the peak $P(O_3)$, although the calculated $P(O_3)$ has more high values at higher NO levels. In addition, both the calculated and modeled $P(O_3)$ are close to zero with low scatter for evening hours whereas the MOPS data are more scattered and include

Direct measurement of ozone production rates in Houston

M. Cazorla et al.

Title Page

Abstract

Introduction

Conclusions

References

Tables

Figures



Back

Close

Full Screen / Esc

Printer-friendly Version

Interactive Discussion



negatives, possibly due to the formation of HNO_3 or other artifacts as discussed previously. Thus, while the NO dependence of the MOPS measurement has qualitative similarities with the NO dependence of both the calculated and the modeled $P(\text{O}_3)$, its shape is closer to that of the modeled $P(\text{O}_3)$ but its magnitude is closer to that of the calculated $P(\text{O}_3)$.

4 Conclusions

The MOPS instrument was able to collect a useful set of ozone production measurements during its first field campaign, SHARP, in Houston during May 2009. Comparisons with $P(\text{O}_3)$ calculated using measured and modeled radicals was made possible by the simultaneous measurement of both the radicals and all the other atmospheric constituents and environmental parameters necessary to constrain a box model.

The analysis presented here shows that $P(\text{O}_3)$ calculated from measurements of HO_x radicals and NO yield better quantitative agreement with the measured $P(\text{O}_3)$ than $P(\text{O}_3)$ obtained from a zero dimensional box model. The peak modeled $P(\text{O}_3)$ values are only half of the measured and calculated values. This result suggests that additional sources of radicals are needed in the model.

In contrast, the NO dependence of the measured $P(\text{O}_3)$ seems to be more like that of the modeled $P(\text{O}_3)$ than that of the calculated $P(\text{O}_3)$, although this conclusion is based on relatively few points. Thus, these results do not adequately resolve the discrepancy in the NO dependence between the $P(\text{O}_3)$ calculated using measured HO_2 and the $P(\text{O}_3)$ using modeled radicals. More observations will be needed to resolve this issue.

These MOPS measurements are the first ones that could be compared to both modeled and calculated $P(\text{O}_3)$. As more measurements are made in different environments by more groups, and as more laboratory studies of the MOPS are undertaken, it is likely that more will be learned about the strengths and weaknesses of the technique. Issues of calibration and artifacts are likely to emerge, as they have for all previous new measurements. However, the SHARP data demonstrate the potential of the MOPS.

Direct measurement of ozone production rates in Houston

M. Cazorla et al.

Title Page

Abstract

Introduction

Conclusions

References

Tables

Figures

◀

▶

◀

▶

Back

Close

Full Screen / Esc

Printer-friendly Version

Interactive Discussion



Direct measurement of ozone production rates in Houston

M. Cazorla et al.

Title Page

Abstract

Introduction

Conclusions

References

Tables

Figures

⏪

⏩

◀

▶

Back

Close

Full Screen / Esc

Printer-friendly Version

Interactive Discussion



From the results presented in this paper, it is clear that the Measurement of Ozone Production Sensor can contribute to the understanding of ozone pollution photochemistry and to the efficacy of air pollution management. The MOPS measures directly the ozone production rate and thus reduces the uncertainties associated with calculating the ozone production rate. These SHARP results also show that the MOPS measurements challenge the understanding of ozone photochemistry found in a chemical mechanism that is widely used in air quality models.

Acknowledgements. The authors thank the College of Earth and Mineral Sciences at the Pennsylvania State University for the Miller Faculty Fellowship, which provided graduate student support for M. C. and funds for the fabrication of MOPS. NSF grant ATM-0209972 supported the initial development of MOPS. We also thank J. Flynn, W. Luke, B. Rappenglück, T. Jobson, and others for providing measurements of NO_x and VOCs used in the modeling.

References

- Appel, K. W., Gilliland, A. B., Sarwar, G., and Gilliam, R. C.: Evaluation for the community multiscale air quality (CMAQ) model version 4.5: Sensitivities impacting model performance Part I – Ozone, *Atmos. Environ.*, 41, 9603–9615, 2007.
- Carslaw, N., Jacobs, P. J., and Pilling, M. J.: Modeling OH, HO₂, and RO₂ radicals in the marine boundary layer 2. Mechanism reduction and uncertainty analysis, *J. Geophys. Res.*, 104, 30257–30273, 1999.
- Cazorla, M. and Brune, W. H.: Measurement of Ozone Production Sensor, *Atmos. Meas. Tech.*, 3, 545–555, doi:10.5194/amt-3-545-2010, 2010.
- Chen, S., Ren, X., Mao, J., Chen, Z., Brune, W. H., Lefer, B., Rappenglück, B., Flynn, J., Olson, J., and Crawford, J. H.: A comparison of chemical mechanisms based on TRAMP-2006 field data, *Atmos. Environ.*, 44, 4116–4125, 2010.
- Environmental Protection Agency (EPA), National Ambient Air Quality Standards for Ozone (Proposed Rule), Federal Register 75, 11 (19 January 2010), 2938–3052, available at: <http://www.epa.gov/glo/fr/20100119.pdf>, 2010.
- Faloona, I. C., Tan, D., Leshner, R. L., Hazen, N. L., Frame, C. L., Simpas, J. B., Harder, H., Martinez, M., Di Carlo, P., Ren, X., and Brune, W. H.: A laser induced fluorescence instrument

**Direct measurement
of ozone production
rates in Houston**

M. Cazorla et al.

Title Page

Abstract

Introduction

Conclusions

References

Tables

Figures

◀

▶

◀

▶

Back

Close

Full Screen / Esc

Printer-friendly Version

Interactive Discussion



for detecting tropospheric OH and HO₂: Characteristics and calibration, *J. Atmos. Chem.*, 47, 139–167, 2004.

Finlayson-Pitts, B. J. and Pitts Jr., J. N.: The chemical basis of air quality: Kinetics and mechanism of photochemical air pollution and application to control strategies, in: *Advances in Environmental Science and Technology*, edited by: Pitts Jr., J. N. and Metcalf, R. L., 75–162, New York, Wiley-Interscience Publication, 1977.

Fox, D. G.: Uncertainty in Air Quality Modeling, *B. Am. Meteorol. Soc.*, 65, 27–36, 1984.

Fuchs, H., Bohn, B., Hofzumahaus, A., Holland, F., Lu, K. D., Nehr, S., Rohrer, F., and Wahner, A.: Detection of HO₂ by laser-induced fluorescence: calibration and interferences from RO₂ radicals, *Atmos. Meas. Tech.*, 4, 1209–1225, doi:10.5194/amt-4-1209-2011, 2011.

Gery, M. W., Whitten, G. Z., Killus, J. P., and Dodge, M. C.: A photochemical kinetics mechanism for urban and regional scale computer modeling, *J. Geophys. Res.*, 94, 12925–12956, 1989.

Gilliland, A. B., Hogrefe, C., Pinder, R. W., Godowitch, J. M., Foley, K. L., and Rao, S. T.: Dynamic Evaluation of Regional Air Quality Models: Assessing Changes in O₃ Stemming from Changes in Emissions and Meteorology, *Atmos. Environ.*, 42, 5110–5123, 2008.

Goliff, W. S. and Stockwell, W. R.: The Regional Atmospheric Chemistry Mechanism, version 2, an update, International conference on Atmospheric Chemical Mechanisms, University of California, Davis, 2008.

Goliff, W. S. and Stockwell, W. R.: The Regional Atmospheric Chemistry Mechanism, version 2.1. Description and Evaluation, *J. Geophys. Res.*, submitted, 2010.

Haagen-Smit, A. J., Bradley, C. E., and Fox, M. M.: Ozone formation in photochemical oxidation of organic substances, *Ind. Eng. Chem.*, 45, 2086–2089, 1953.

Hard, T. M., O'Brien, R. J., Chan, C. Y., and Mehrabzadeh, A. A.: Tropospheric free radical determination by FAGE, *Environ. Sci. Technol.*, 18, 768–777, 1984.

Hofzumahaus, A., Roher, F., Lu, K., Bohn, B., Brauers, T., Chang, C.-C., Fuchs, H., Holland, F., Kita, K., Kondo, Y., Li, X., Lou, S., Shao, M., Zeng, L., Wahner, A., and Zhang, Y.: Amplified Trace Gas Removal in the Troposphere, *Science*, 324, 1702–1704, 2009.

Jobson, B. T., Alexander, M. L., Maupin, G. D., and Muntean, G. G.: On-line analysis of organic compounds in diesel exhaust using a proton transfer reaction mass spectrometer (PTR-MS), *Int. J. Mass Spectrom.*, 245, 78–89, 2005.

Kanaya, Y., Cao, R., Akimoto, H., Fukuda, M., Komazaki, Y., Yokouchi, Y., Koike, M., Tanimoto, H., Takegawa, N., and Kondo, Y.: Urban photochemistry in central Tokyo: 1. Observed

**Direct measurement
of ozone production
rates in Houston**

M. Cazorla et al.

Title Page

Abstract

Introduction

Conclusions

References

Tables

Figures

◀

▶

◀

▶

Back

Close

Full Screen / Esc

Printer-friendly Version

Interactive Discussion



- and modeled OH and HO₂ radical concentrations during the winter and summer of 2004, *J. Geophys. Res.*, 112, D21312, doi:10.1029/2007JD008670, 2007.
- Kleinman, L. I.: The dependence of tropospheric ozone production rate on ozone precursors, *Atmos. Environ.*, 39, 575–586, 2005.
- 5 Lefer, B. L., Rappenglück, B., Olaguer, E. P., Brune, W., Stutz, J., Dibb, J. E., Ren, X., Herndon, S. C., Jobson, T. B., Mount, G., Yu, X. Y., Griffin, R., Thomas, S., Shauck, M., Huey, L. G., Zhang, R., Jimenez, J. L.: First Results of the Study of Houston Atmospheric Radical Precursors (SHARP), 12th Conference on Atmospheric Chemistry, American Meteorological Society, 2010.
- 10 Leuchner, M. and Rappenglück, B.: VOC source–receptor relationships in Houston during TexAQS-II, *Atmos. Environ.*, 44, 4056–4067, 2010.
- Logan, J. A., Prather, M. J., Wofsy, S. C., and McElroy, M. B.: Tropospheric Chemistry: A global perspective, *J. Geophys. Res.*, 86, 7210–7254, 1981.
- Luke, W. T., Kelley, P., Lefer, B. L., and Flynn, J. H.: Measurements of reactive nitrogen compounds (NO, NO_x, NO_y) during SHARP, 12th Conference on Atmospheric Chemistry, American Meteorological Society, 2010.
- 15 Martinez, M., Harder, H., Kovacs, T. A., Simpas, J. B., Bassis, J., Leshner, R., Brune, W. H., Frost, G. J., Williams, E. J., Stroud, C. A., Jobson, B. T., Roberts, J. M., Hall, S. R., Sheter, E., Wert, B., Fried, A., Alicke, B., Stutz, J., Young, V. L., White, A. B., and Zamora, R. J.: OH and HO₂ concentrations, sources, and loss rates during the Southern Oxidants Study in Nashville, Tennessee, summer 1999, *J. Geophys. Res.*, 108, 4617, doi:10.1029/2003JD003551, 2003.
- 20 McCarthy, J. E.: Ozone Air Quality Standards: EPA’s Proposed January 2010 Revisions, Congressional Research Service, available at: www.fas.org/sgp/crs/misc/R41062.pdf, 2010.
- 25 National Research Council (NRC), Rethinking the ozone problem in urban and regional air pollution, Natl. Acad. Press, 109–186, 1991.
- Ren, X., Harder, H., Martinez, M., Leshner, R., Oliger, A., Simpas, J., Brune, W., Schwab, J., Demerjian, K., He, Y., Zhou, X., and Gao, H.: OH and HO₂ Chemistry in the urban atmosphere of New York City, *Atmos. Environ.*, 37, 3639–3651, 2003.
- 30 Ren, X., Harder, H., Martinez, M., Faloona, I. C., Tan, D., Leshner, R. L., Di Carlo, P., Simpas, J. B., and Brune, W. H.: Interference testing for atmospheric HO_x measurements by laser-induced fluorescence, *J. Atmos. Chem.*, 47, 169–190, 2004.
- Seinfeld J. H. and Pandis, S. N.: Atmospheric chemistry and physics from air pollution to climate

Direct measurement of ozone production rates in Houston

M. Cazorla et al.

Title Page

Abstract

Introduction

Conclusions

References

Tables

Figures

◀

▶

◀

▶

Back

Close

Full Screen / Esc

Printer-friendly Version

Interactive Discussion



change, second edition, Wiley, NJ, 204–274, 2006.

Shirley, T. R., Brune, W. H., Ren, X., Mao, J., Leshner, R., Cardenas, B., Volkamer, R., Molina, L. T., Molina, M. J., Lamb, B., Velasco, E., Jobson, T., and Alexander, M.: Atmospheric oxidation in the Mexico City Metropolitan Area (MCMA) during April 2003, *Atmos. Chem. Phys.*, 6, 2753–2765, doi:10.5194/acp-6-2753-2006, 2006.

Stockwell, W. R., Kirchner, F., and Kuhn, M.: A new mechanism for regional atmospheric chemistry modeling, *J. Geophys. Res.*, 102, 25847–25879, 1997.

Texas Commission On Environmental Quality, 2009 Air Pollution Events, available at: <http://www.tceq.state.tx.us/compliance/monitoring/air/monops/sigevents09.html>, 2011.

Wainman, T., Wescheler, C. J., Liou, P. J., and Zhang, J.: Effects of surface type and relative humidity on the production and concentration of nitrous acid in a model indoor environment, *Environ. Sci. Technol.*, 35, 2200–2206, 2001.

Willmott, C. J.: On the validation of models, *Phys. Geogr.*, 2, 184–194, 1981.

**Direct measurement
of ozone production
rates in Houston**

M. Cazorla et al.

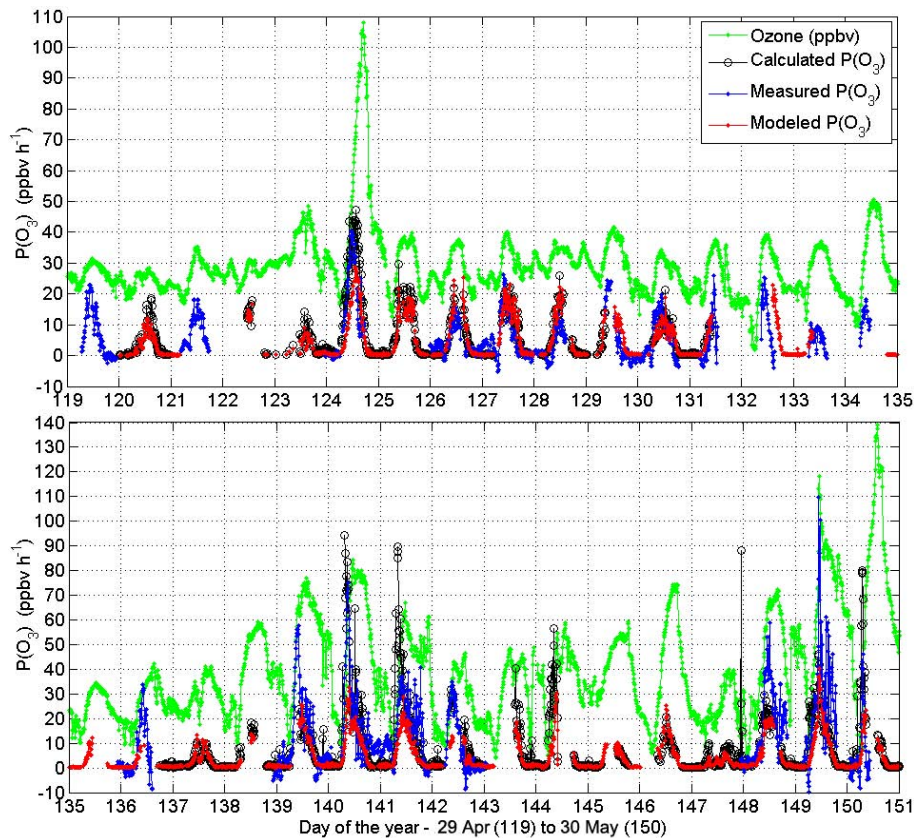


Fig. 1. Time series from 29 April (day 119) to 30 May (day 150) 2009 for ambient ozone (green dots), calculated $P(\text{O}_3)$ from measured radicals (black circles), measured $P(\text{O}_3)$ with the MOPS (blue dots) and modeled $P(\text{O}_3)$ from the RACM2 mechanism (red dots).

Title Page

Abstract

Introduction

Conclusions

References

Tables

Figures

◀

▶

◀

▶

Back

Close

Full Screen / Esc

Printer-friendly Version

Interactive Discussion



**Direct measurement
of ozone production
rates in Houston**

M. Cazorla et al.

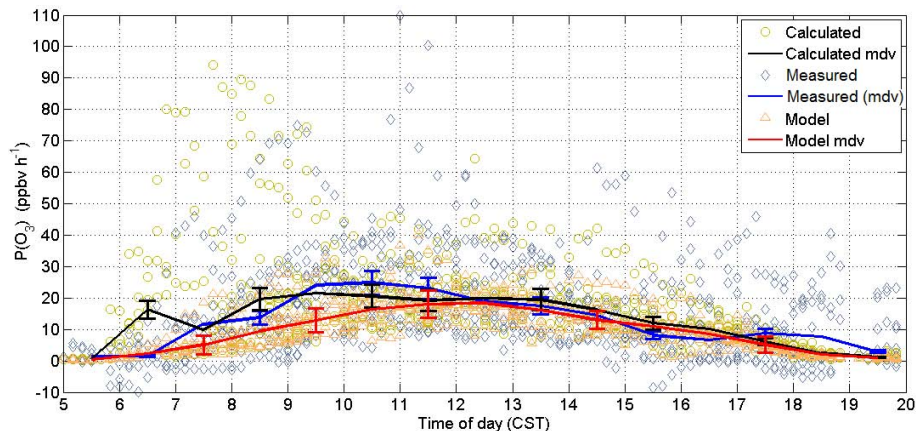


Fig. 2. Overlapping 10-min points and median diurnal variation (mdv) for calculated (yellow circles and black line), measured with the MOPS (light blue diamonds and blue line) and modeled $P(\text{O}_3)$ (orange triangles and red line). Comparison is done for overlapping data only during daylight hours in Central Standard Time (CST). Error bars are 1σ based on measurement uncertainty for the GTHOS and MOPS instruments and on calculated model uncertainty at different times of the day.

[Title Page](#)[Abstract](#)[Introduction](#)[Conclusions](#)[References](#)[Tables](#)[Figures](#)[◀](#)[▶](#)[◀](#)[▶](#)[Back](#)[Close](#)[Full Screen / Esc](#)[Printer-friendly Version](#)[Interactive Discussion](#)

Direct measurement of ozone production rates in Houston

M. Cazorla et al.

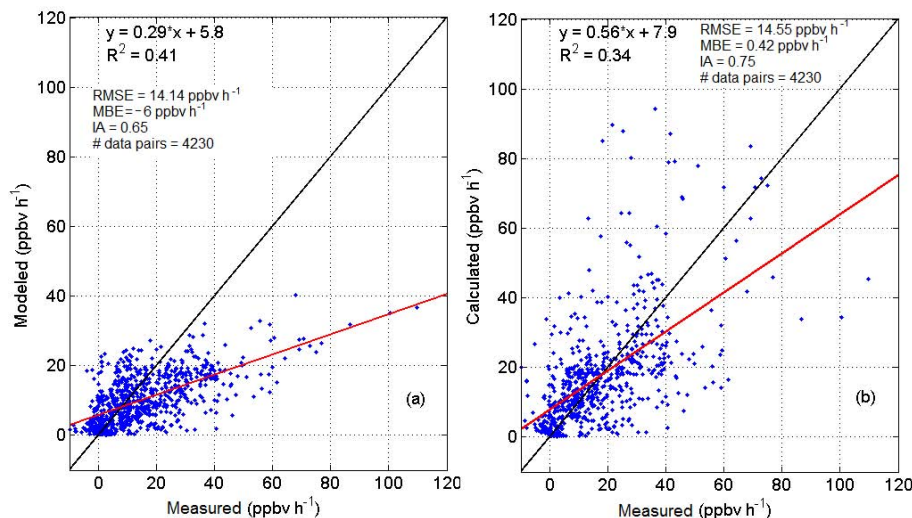


Fig. 3. Scatter plots showing the correlation between **(a)** modeled and measured $P(\text{O}_3)$ and **(b)** calculated versus measured $P(\text{O}_3)$. On both plots the black line is the 1:1 line while the red line comes from the linear regression between y axis (calculated or modeled) and x axis (measured with the MOPS) $P(\text{O}_3)$ values. Errors in slope and intercept are 1.38 % and 32.5 % for **(a)**; and 3.05 % and 71.6 % for **(b)**.

[Title Page](#)
[Abstract](#)
[Introduction](#)
[Conclusions](#)
[References](#)
[Tables](#)
[Figures](#)
[◀](#)
[▶](#)
[◀](#)
[▶](#)
[Back](#)
[Close](#)
[Full Screen / Esc](#)
[Printer-friendly Version](#)
[Interactive Discussion](#)


Direct measurement of ozone production rates in Houston

M. Cazorla et al.

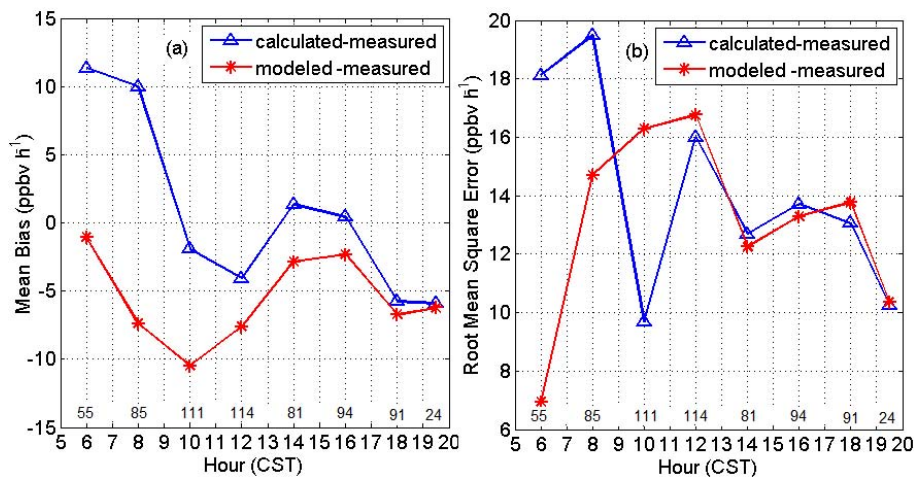


Fig. 4. (a) Mean Bias Error (MBE) and (b) Root Mean Square Error (RMSE) for calculated vs. measured data (blue line and open triangles) and for modeled vs. measured data (red line and stars) binned by hour of the day. The number of binned pairs of data is indicated on top of the x-axis values.

Title Page

Abstract

Introduction

Conclusions

References

Tables

Figures

◀

▶

◀

▶

Back

Close

Full Screen / Esc

Printer-friendly Version

Interactive Discussion



**Direct measurement
of ozone production
rates in Houston**

M. Cazorla et al.

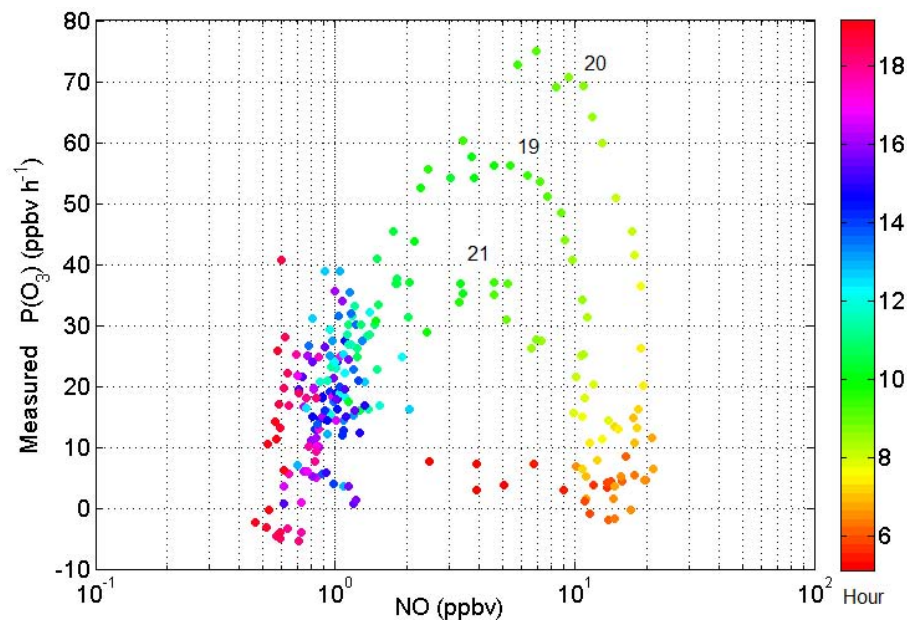


Fig. 5. Measured $P(\text{O}_3)$ in NO space for the high ozone episode that started on 19 May, developed on 20 May and subsided on 21 May, 2009 in Houston. The color scale corresponds to hour of the day. The number on top of every curve is the date in May.

Title Page

Abstract

Introduction

Conclusions

References

Tables

Figures

◀

▶

◀

▶

Back

Close

Full Screen / Esc

Printer-friendly Version

Interactive Discussion



**Direct measurement
of ozone production
rates in Houston**

M. Cazorla et al.

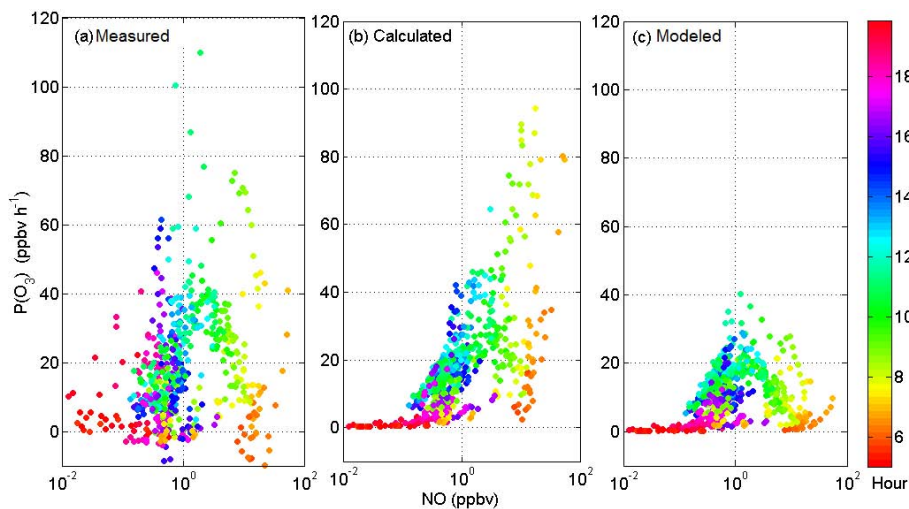


Fig. 6. $P(\text{O}_3)$ in NO space **(a)** measured by the MOPS, **(b)** calculated and **(c)** modeled for overlapping points only and daylight hours. The color scale corresponds to hour of the day.

Title Page

Abstract

Introduction

Conclusions

References

Tables

Figures

◀

▶

◀

▶

Back

Close

Full Screen / Esc

Printer-friendly Version

Interactive Discussion

